An eSnake model for medical image segmentation *

LÜ Hongyu[1], YUAN Kehong[2], BAO Shanglian[1], ZU Donglin[1] and DUAN Chaijie[1] **

(1. The Research Center for Tumor Diagnosis and Therapeutical Physics & Beijing Key Laboratory of Medical Physics and Engineering, Beijing 100871, China; 2. Key Laboratory of Pure and Applied Mathematics, School of Mathematical Sciences, Peking University, Beijing 100871, China)

Received August 23, 2004; revised November 2, 2004

Abstract A novel scheme of external force for detecting the object boundary of medical image based on Snakes (active contours) is introduced in the paper. In our new method, an electrostatic field on a template plane above the original image plane is designed to form the map of the external force. Compared with the method of Gradient Vector Flow (GVF), our approach has clear physical meanings. It has stronger ability to conform to boundary concavities, is simple to implement, and reliable for shape segmenting. Additionally, our method has larger capture range for the external force and is useful for medical image preprocessing in various applications. Finally, by adding the balloon force to the electrostatic field model, our Snake is able to represent long tube-like shapes or shapes with significant protrusions or bifurcations, and it has the specialty to prevent Snake leaking from large gaps on image edge by using a two-stage segmentation technique introduced in this paper. The test of our models proves that our methods are robust, precise in medical image segmentation.

Keywords: image segmentation, eSnake, external force, electrostatic field, balloon force.

Deformable model is a curve or a surface driven partial differential equations (PDE) method for image segmentation and pattern recognition. Two types of deformable models have been developed previously. One is the parametric deformable model proposed by Kass et al.[1], which formulates the curve explicitly in the parametric form. The other is the geometric deformable model, which implicitly characterizes the curve by a level set function developed by Osher, Sethian and implemented by Malladi[2]. Hybrid methods are proposed to combine the techniques of both models, such as the Geodesic Active Contour model proposed by Caselles[3].

The parametric deformable model, also known as the Snakes or active contour, is aiming at minimizing a specified energy function subject to some constraints. Although the level set method is an attractive mathematical framework and it can govern the curvature-dependent front evolution, implicit formulations are not nearly as convenient as the explicit ones, because parametric formulations incorporate additional control mechanisms. In the cases of poor contrast boundaries, large gaps in boundaries or high noise commonly existing in medical, infrared and remote sensing images, the parametric model is a better choice[4,5].

Taking advantage of edge detection techniques, the parametric deformable model becomes mature and robust for practical usage in medical image segmentation and pattern recognition. The research is mainly focused on three areas, the curve representation related to internal force[6—8], the external force and energy minimization methods[9—11]. The famous external force model includes Gradient, Balloon[1], Distance maps[12] and Gradient Vector Flow (GVF)[13,14], etc. The problem in modeling external force is to find one kind of force that can possess large range capture, push the curves to the concavities or convexes and stop the evolving Snakes at the edge gaps. It is a dilemma to construct one optimized model for external force. Compared with other external forces, the GVF model partly overcomes these obstacles by taking the concepts from optical flow. The shortcoming of GVF is that it is difficult to understand and it has no physical and geometric meanings. Moreover, GVF is impossible to push or pull the contour to the significant concavities or convexes. GVF also lacks the power to stop the contour at large gaps in some conditions.

Motivated by the basic ideas of GVF, we designed a model of external force which has clear physical meanings. This approach utilizes a template plane above the original image plane. Then, the pixels at

* Supported by National Natural Science Foundation of China (Grant Nos. 10275003 and 10175004), and Natural Science Foundation of Beijing (Grant No. 3011002)

** To whom correspondence should be addressed. E-mail: bao@pku.edu.cn

the image edge are regarded as point electric charges, which contribute the electrostatic potential on the template plane to the forming of the electrostatic field. The precision of segmentation is desirable. In most cases, there are no requests for changing the parameters of the Snake. Furthermore, the special vector field coming from this model is helpful for thinning the monochromatic images, assisting the design of anisotropic filters, and analyzing the image optical flow. In order to make the contour conform to the shapes with complex topology such as long tube-like shapes or shapes with significant branching or protrusions, another model structured by joining a geometric based balloon force is also proposed in the paper, which only needs to take a few efforts to find the suitable parameters, such as regulating slightly the weight of the balloon force sometimes. The algorithm of explicit finite difference method is applied for the numerical solution and we found that the computing time is stable for most usages if all parameters are appropriate according to the constraints described above. Since the model we developed here is mainly based on electrostatic field, we call it eSnake model.

1 Analysis of GVF and the electrostatic field description

A traditional Snake is a curve or contour with the formulation of $\boldsymbol{X}(s)=[x(s), y(s)]$, $s\in[0, 1]$, which moves through the spatial domain of an image to a local area with minimized energy. For a normal grey-level image $I(x, y)$, the energy of the Snake can be expressed as:

$$E_{\text{total}}=\int_0^1[E_{\text{Internforce}}(\boldsymbol{X}(s))+E_{\text{Externforce}}(\boldsymbol{X}(s))]\,\mathrm{d}s, \quad (1)$$

$$E_{\text{Internforce}}(\boldsymbol{X}(s))=\frac{1}{2}[\alpha|\boldsymbol{X}'(s)|^2+\beta|\boldsymbol{X}''(s)|^2], \quad (2)$$

$$E_{\text{Externforce}}=-|\nabla[G_\sigma(x, y)\otimes I(x, y)]|^2, \quad (3)$$

where α and β in Eq. (2) are weighting parameters that control the Snake's tension and rigidity. $G_\sigma(x, y)$ is the two-dimensional Gaussian function with standard deviation σ, and ∇ is the gradient factor. According to the Euler-Lagrange condition of variation calculus, the minimum of E_{total} which represents the final stable energy of a Snake must satisfy the following equation:

$$\alpha\boldsymbol{X}''(s)-\beta\boldsymbol{X}''''(s)-\nabla E_{\text{Externforce}}(s)=0, \quad (4)$$

where $\nabla E_{\text{Externforce}}(s)=-F_{\text{Extern}}(s)$.

It is easy to apply the finite difference method (FDM) in time domain to find a solution of Eq. (4). Because E_{total} is usually close to the largest value at the beginning of the curve evolution, we have

$$\frac{\partial\boldsymbol{X}(s, t)}{\partial t}=\alpha\frac{\partial^2\boldsymbol{X}(s, t)}{\partial s^2}-\beta\frac{\partial^4\boldsymbol{X}(s, t)}{\partial s^4}+F_{\text{Extern}}(s, t). \quad (5)$$

In GVF, the external force is usually generated by the equation

$$\varepsilon=\iint\mu(u_x^2+u_y^2+v_x^2+v_y^2)+|\nabla f|^2|v-\nabla f|^2\mathrm{d}x\mathrm{d}y. \quad (6)$$

In Eq. (5), $F_{\text{extem}}(x, y)=[u(x, y), v(x, y)]$, and in Eq. (6), μ is a weighting parameter for governing the tradeoff between the first and second terms in the integrand. Equation (6) creates an energy field containing both degree of divergence and curl for a vector field. Using the calculus of variation and finite difference method again, $F_{\text{extem}}(x, y)$ can be calculated according to

$$u_t(x, y, t)=\mu\nabla^2u(x, y, t)-[u(x, y, t)-f_x(x, y)]\cdot[f_x^2(x, y)+f_y^2(x, y)], \quad (7)$$

$$v_t(x, y, t)=\mu\nabla^2v(x, y, t)-[v(x, y, t)-f_y(x, y)]\cdot[f_x^2(x, y)+f_y^2(x, y)]. \quad (8)$$

It is shown that the meaning of the GVF is not obvious, and there is no more progress after Xu and Prince[5] developed GGVF (generalized gradient vector flow). Due to the complexity of GVF itself, the GGVF does not show its stable numerical solution.

In Ivins's PhD thesis[15], he structured a force

$$E_{\text{Exernforce}}(\boldsymbol{X})=\frac{k}{|\boldsymbol{i}-\boldsymbol{X}|^2}, \quad (9)$$

which is similar to an electrostatic force. However, as an illustration, external force energy in Snakes is unusable because the infinite value can be produced when $\boldsymbol{i}(x, y)=\boldsymbol{X}(x, y)$.

In the 2D image space, there were several attempts to solve the problem, but the results often had disconnected or false edges in edge detection. Therefore, people have to find another method to solve the problem with an acceptable precision.

2 Electrostatic field of eSnake model

The progress in our paper is that we propose a

physical model to overcome the infinite problem in Eq. (9) by using an electrostatic field formed above the plane of the target image. The principle is showed in Fig. 1.

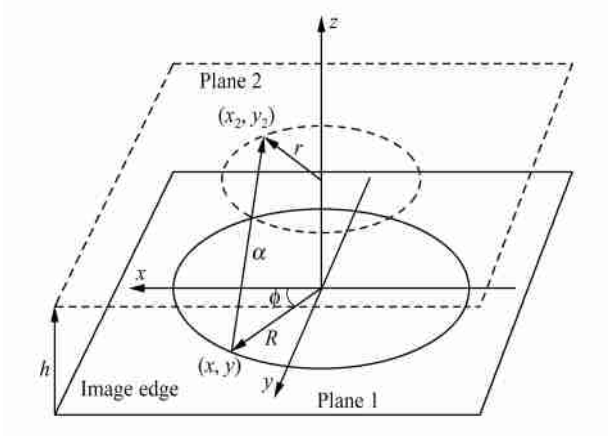

Fig. 1. Schematic diagram for calculation of electrostatic field of eSnake.

Suppose each pixel in the discrete 2D image domain is a unit electric-charge, the potential $\varphi_{\text{Plane2}}(x_2, y_2)$ on the plane by the pixel (x, y) can be derived:

$$\varphi_{\text{Plane2}}(x_2, y_2) = \frac{e}{4\pi\varepsilon_0}\sum \frac{1}{\sqrt{(x_2-x)^2+(y_2-y)^2+h^2}}. \tag{10}$$

Therefore, the distribution of the electric field intensity between (x_1, y_1) and (x_1, y_1) can be described as:

$$E_{x_2}(x_2, y_2) = \frac{\Delta\varphi(x_2, y_2)}{\Delta x_2} = \frac{\varphi((x_2+1), y_2) - \varphi((x_2-1), y_2)}{2}, \tag{11}$$

$$E_{y_2}(x_2, y_2) = \frac{\Delta\varphi(x_2, y_2)}{\Delta y_2} = \frac{\varphi(x_2, (y_2+1)) - \varphi(x_2, (y_2+1))}{2}, \tag{12}$$

which is an explicit expression of the external energy, and it can reach very high accuracy if the time step taken in the calculation is small enough. Furthermore, the method is fast enough for the calculation and easy for explaining the result.

During the model development, the most important parameter h is defined as the distance between two planes. In the case of $h>0$, $\varphi_{\text{Plane2}}(x', y')$ is very sensitive to the value of h. Since the distance between pixels is at least equal to one in the image and the potential field is usually symmetric, different h values are tested with three small circle charges whose radii along the x axis are $R=0.5$, $R=1$, and $R=5$, respectively, (Fig. 1) which is used to solve Eq. (10) for estimation of the h volumes. E_x can be computed from $dU(x)/dx$. The results are shown in Fig. 2.

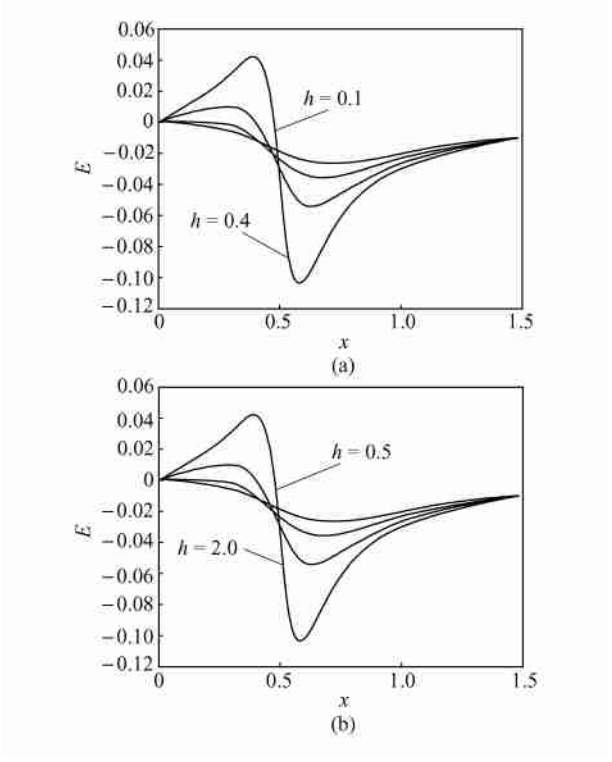

Fig. 2. Results of the calculated E_x with different h and R values. (a) Plots of E_x with $h=0.1$, 0.2, 0.5, 0.4, $R=0.5$; (b) plots of E_x with $h=0.5$, 1.0, 1.5, 2.0, $R=5$.

The position on the x axis where Ex equals 0 indicates that the edge point is found by Snakes. The testing results show that the smaller h is, the more accurately it represents the position of the circle edge. At the same time, the smaller the value of h is, the less smooth the edges of the electric field are. From the tests, we estimate that h should be in the range of (0, 1]. For example, when $h=0.2$, the detecting precision is within one pixel, which is a trade off result between adaptive shape and edge detection accuracy. In our experiments, h was taken as 0.2, 0.5 and 1.0. Figure 3 shows the potential surface and the electrostatic field distribution obtained from our method.

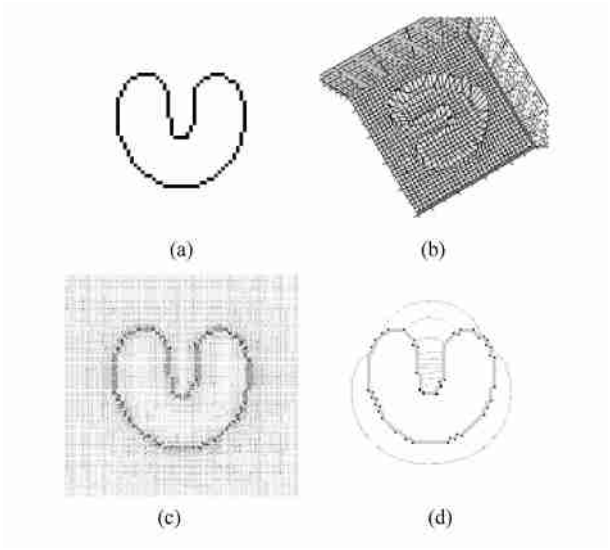

Fig. 3. Example of the eSnake model principle. (a) Original image; (b) potential surface; (c) electrostatic field; (d) curve evolving process.

3 Balloon force in eSnake

Although it can give better segmentation results than GVF, the electrostatic force model we established still has a similar problem in GVF. It lacks the ability to move along long tubular shapes or shapes with significant branches and protrusions. To overcome these drawbacks, a balloon force is added. Cohen introduced a pressure force which has the feature like an inflating or deflating balloon[10]. It can be expressed as:

$$F_{\text{Balloon}} = \lambda n(s), \tag{13}$$

where $n(s)$ is a unit vector normal to the curve at point $v(s)$ and λ is the amplitude of the force. There are two kinds of balloon force: geometry based model and region based model[4,15] derived from the former one. Region based balloon force is impossible to operate on monochromatic images and is difficult to work well for identifying the shape region in which the grey level is not very homogeneous. We choose the geometry based balloon model by simply expressing it as:

$$n_x = \frac{\Delta y}{|\Delta y|}, \quad n_y = -\frac{\Delta x}{|\Delta x|}. \tag{14}$$

This formula gives satisfactory results from the testing.

Taking both Eq. (11) and Eq. (14) as the external forces and apply the explicit finite difference method, the equations for our Snake can be established as:

$$\frac{x(t+\Delta t)-x(t)}{\Delta t} = \alpha x''(t) - \beta x''''(t) + \gamma E_x(x,y) + \lambda n_x(x(t),y(t)), \tag{15}$$

$$\frac{y(t+\Delta t)-y(t)}{\Delta t} = \alpha y''(t) - \beta y''''(t) + \gamma E_y(x,y) + \lambda n_y(x(t),y(t)). \tag{16}$$

The procedure of the solution has two steps to pull the contour leaking out of the large gap of the image edges. In the first step, we took a large γ, and let λ be smaller than γ, e.g. $\gamma=0.05$ and $\lambda=0.008$. In the second step, we took γ as a smaller value and let λ equal 0, e.g. $\gamma=0.01$ and $\lambda=0$, which give the results that the electric outside field is stronger than the inside one. The structure keeps the contour leaking out from the gaps in the image, which can not be driven back. The structure makes the parameters more stable and let the structured eSnake be more robust.

4 Experiments and results

4.1 Method of testing

Edge detection plays an important role in the segmentation by the Snake. Gradient, Laplacian, Prewitt and Sobel filters with thresholds, as well as the anisotropic filters were used for the edge detection. In our testing, Canny detector[16] was chosen due to its optimal performance. Two kinds of Canny detectors were used: one was standard; the other was a simplified algorithm which gives an edge with thick lines (http://www.pages.drexel.edu/~weg22). The contour of eSnake is located close to the middle of the thick lines at the edge, which is specified by charge attraction force domain in the electrostatic field.

Guéziec[17] pointed out that although many researchers had published their applications in this field, only a few of them were reliable and successful in practice, because they paid more attention to innovation than to the algorithm in practice[17]. In practice, the reliability is more important. Therefore, we give a full test of our algorithm with various kinds of images. In our tests, $\beta=0$ is supposed because the smoothing ability is not the feature we pursue and the fourth order of derivative exerts little impact on the contour. In our tests, if there was not any special declaration, the parameters were chosen as $\Delta t=0.1$, $\alpha=0.5$, $\gamma=0.05$, $\lambda=0.008$, $h=0.2$.

4.2 eSnake with electrostatic field

The large capture range, the ability to stop at

the edge gaps of the images are indicated by the results of Fig. 4. Fig. 5 (a) and (b) show that our model is better than the GVF model in penetrating into concave and convex edges. It can be seen from Fig.5(c) and (d) that in the stopping curve at large gaps, our model has poorer performance but it turns into a merit when adding balloon force to eSnake. The original image in Fig. 6(a) has more noise, which was treated with a Gaussian filter, then passed with the simplified Canny filter. In the condition of $h=0.5$, the contour line is located in the middle of the edge. A comparison between GGVF and eSnake is shown in Fig 7. Even in the case of $h=1.0$, eSnake gives the better result for detecting the concavity in the top region of the image.

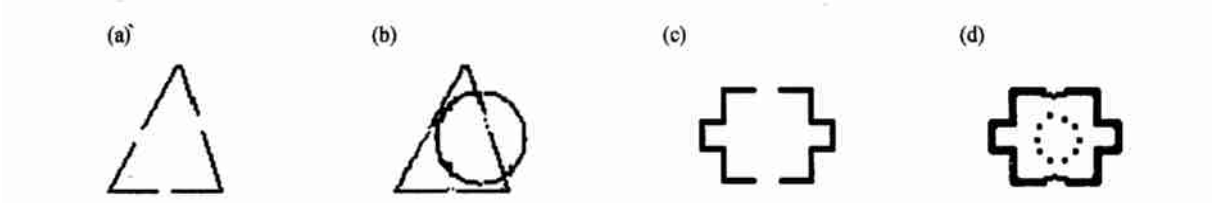

Fig. 4. Example of the eSnake model. (a) Original image; (b) result of eSnake; (c) original image; (d) result of eSnake.

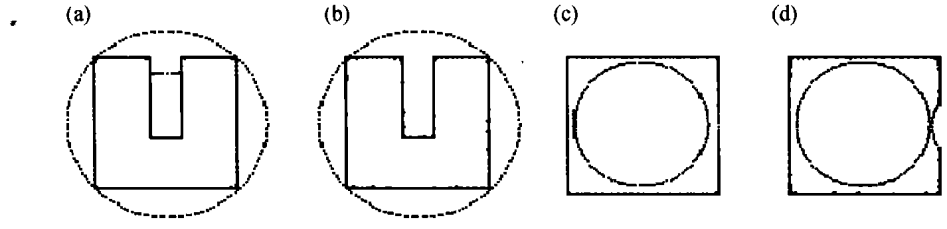

Fig. 5. Example of the eSnake model. (a) Result of GVF; (b) result of eSnake; (c) result of GVF; (d) result of eSnake.

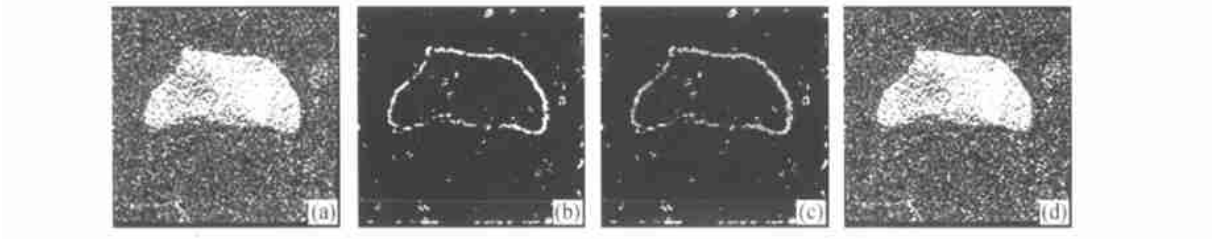

Fig. 6. Bladder image processing using the eSnake model. (a) Bladder image of MRI; (b) detected edges and initial Snake; (c) result on edges; (d) result on image. $h=0.5$.

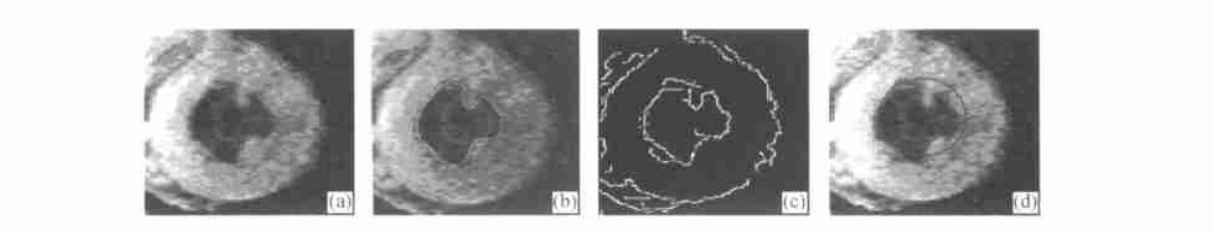

Fig. 7. Heart image processing using the eSnake model. (a) Heart image of MRI; (b) results of GGVF; (c) detected edges; (d) result of eSnake. $h=1.0$.

4.3 eSnake with Balloon

We used the two stages for segmentation tests with parameters $\gamma=0.01$ and $\lambda=0$. All the other parameters are the same as those described in section 4.1 if they are not specified. Fig. 8 shows that the eSnake with balloon force conforms to long tube-like shapes or shapes with significant protrusions and bifurcations, as well as the shapes with sophisticate geometric boundaries. Fig. 9 gives examples of two stages eSnake segmentation and Fig. 9(b) shows a large gap on the edge. In Step 1, the curve goes out of the boundary and in Step 2, it is pulled back.

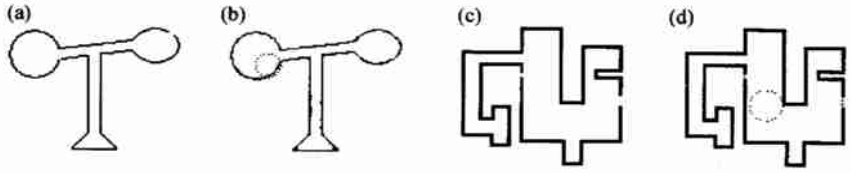

Fig. 8. Example of the eSnake model. (a) Original image; (b) result of eSnake; (c) original image; (d) result of eSnake. For (a) and (b) $\lambda=0.01$ in step 1; for (c) and (d) $\gamma=0.03$, $\lambda=0.007$ in step 1.

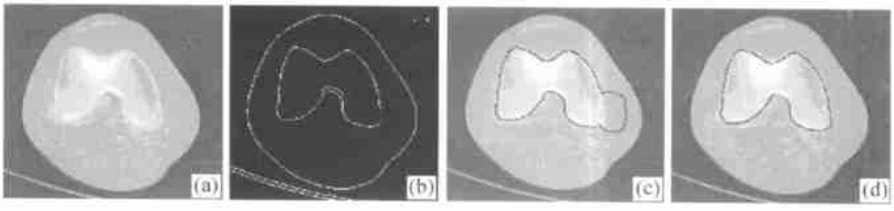

Fig. 9. CT image processing using the eSnake model. (a) Original CT image; (b) detected edges with initial Snake; (c) result of step 1; (d) final result of step 2. In step 1, $\lambda=0.006$.

5 Conclusion

We have introduced a new external force model and named it an eSnake, which has clear physical meanings for the Snakes in 2-D space domain. The force was calculated as an electrostatic field on a template plane above the original image plane. We find that it can allow a flexible initialization of the active contour, encourage converging to boundary concavities and convexes, and minimize the effect of spurious edges. Cooperating with the Balloon force, eSnake is capable of moving through the long tube-like shapes or shapes with significant protrusions and bifurcations. By adapting two stages segmentation technique, eSnake can stop the growing curves at the large gaps. From various experiments, it is demonstrated that our method is reliable, precise and robust for shaping complex boundaries. In addition, our algorithm is simple in practical usage.

Further investigation will be emphasized on applying our scheme to the segmentation of the multipliable objects together with the study of the 3-D surface segmentation. In particular, the vector map created by our electrostatic field model might be useful for image preprocessing such as image thinning, filtering and optical flow research, which is useful in medical image processing.

References

1 Kass M., Witkin A. and Terzopoulos D. Snakes: Active contour models. International Journal of Computer Vision, 1988, 1: 321—331.
2 Malladi R., Sethina J. and Vemuri B. Shape modeling with front propagation: a level set Approach. IEEE Trans. on Pattern Analysis and Machine Intelligence, 1995, 17(2): 18—175.
3 Caselles V. Geodesic active contour. International Journal of Computer Vision, 1997, 22(1): 61—79.
4 McInerney T. T. T-Snakes: Topology adaptive snakes. Medical Image Analysis, 2000, 4: 73—91.
5 Xu C. and Prince J. L. Generalized gradient vector flow external forces for active contours. Signal Processing, 1998, 71(2): 131—139.
6 Brigger P., Hoeg J. and Unser M. B-Spline snakes: A flexible tool for parametric contour detection. IEEE Trans. on Image Processing, 2000, 9(9): 1484—1496.
7 Cootes T. F. and Taylor C. J. Using grey-level models to improve active shape model search. In: Proceedings of the 12th IAPR International Conference on Computer Vision & Image Processing, 1994, 63—67.
8 Lobregt S. and Viergever M. A. A discrete dynamic contour model. IEEE Trans. on Medical Imaging, 1995, 14(1): 12—24.
9 Amini A. A., Weymouth T. E. and Jain R. C. IEEE Trans. on Pattern Analysis and Machine Intelligence. 1990, 12(9): 855—867.
10 Cohen L. D. and Cohen I. Finite-element methods for active contour models and balloons for 2-D and 3-D images. IEEE trans. on Pattern Analysis and Machine Intelligence, 1993, 15(11): 1131—1147.
11 Williams D. J. and Shah M. A. Fast algorithm for active contours. In: the Third International Conference on Computer Vision, Osaka, Japan, 1990, 592—595.
12 Cohen L. D. and Cohen I. Finite-element methods for active contour models and balloons for 2-D and 3-D images. IEEE Trans. on Pattern Analysis and Machine Intelligence, 1993, 15(11): 1131—1147.
13 Xu C., Pham D. L. and Prince J. L. Medical Image Segmentation Using Deformable Models. Handbook of Medical Imaging. Bellingham, Wash: SPIE Press, 2000, 129—174.
14 Xu C. and Prince J. L. Snakes, shapes, and gradient vector flow. IEEE Trans. on Image Processing, 1998, (3): 359—369.
15 Ivins J. and Porrill J. Active region models for segmenting textures and colours. Image and Vision Computing, 1995, 13(5): 431—438.
16 Canny F. J. Acomputational approach to edge detection. IEEE Trans. on Pattern Analysis and Machine Intelligence, 1986, 8(6): 679—698.
17 Guéziec A. Tracking pitches for broadcast television. Computer, 2002, 35(3): 38—43.